JOURNAL OF SOLID STATE CHEMISTRY 68, 128–131 (1987)

Solid State Chemistry of Polytungstic Acids and Their Salts

I. Preparation of Fluorescently Pure Tungstosilicic Acid with a Cation-Exchange Membrane Electrolytic Method

LIGAO CHEN, YILUM LIU,* AND YUANZHU CHEN†

Department of Physics, University of Science and Technology of China, Hefei, Anhui, The People's Republic of China

Received March 11, 1986; in revised form July 7, 1986

Fluorescently pure tungstosilicic acid was prepared by electrolysis with a cation-exchange membrane used as an electrolyzer, and the acid was studied with thermal analysis, UV, IR, and emission spectroscopy, and conductance measurement techniques. The results showed that this method has the advantages of simplicity, low consumption of starting materials, and providing a product of high purity. Anhydrous tungstosilicic acid decomposed at 435–525°C, and its ionic conductivity in the solid state was $(3 \pm 1) \times 10^{-3}$ ohm^{-1} cm^{-1} at 25°C. © 1987 Academic Press, Inc.

1. Introduction

Kepert (*1*) and Kazanskii *et al.* (*21*) have reviewed the chemistry of the polytungstic acids and their salts, putting emphasis on their solution chemistry, but giving little attention to their solid state chemistry. Because of their use in phosphors as starting materials (*3*) and in antileukemia drugs (*4*), great attention has been paid to them. However, important progress in the preparation of tungstosilicic acids (TSAs) has not been made, and some of their properties, especially their solid state properties, are not yet understood.

Preparation of TSA by the cation-exchange membrane electrolytic method (CEMEM) (*5*) does not have the disadvantages of the mineral acidification method and the ion-exchange method (*6*); nevertheless, no detailed procedures for this method are given in the literature, and from the methods in (*5*) we could not obtain TSAs of fluorescent purity.

This paper reports a refined CEMEM for the preparation of fluorescently pure TSAs and also gives some of their solid state properties.

2. Experimental

2.1. Preparation of Fluorescently Pure TSA

A diagram of the CEMEM cell is shown in Fig. 1. The thickness of the cation-exchange membrane may range from 0.3 to 0.6 mm; it has a typical resistance of 11 to 22 ohm^{-1}. While the electrolysis was in progress, the cathode solution was slowly and continuously siphoned from the negative side of the cell into a container; at the same

* Present address: Department of Chemistry, Northwest University, Xian, Shanxi, The People's Republic of China.

† Present address: Institute of Materials Structure of Fujian, Academia Sinica, Fuzhou, Fujian, The People's Republic of China.

0022-4596/87 $3.00

Copyright © 1987 by Academic Press, Inc.
All rights of reproduction in any form reserved.

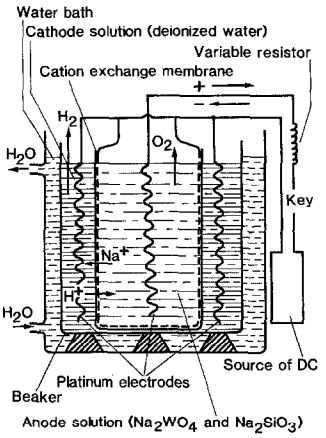

FIG. 1. Diagram of the electrolytic setup.

time deionized water was dropped into the cathode and anode solutions (not shown in Fig. 1). The anode solution temperature was kept below 40°C with running water. The direct current and voltage were adjusted to the concentration of the cathode solution and to the resistances of the electrodes and the membrane; electrolysis continued until the anode solution was in the range of approximately 0.4–0.6 pH. Sodium ions were removed from the anode solution and hydrogen ions entered the anode solution from the cathode solution by a cation-exchange membrane under the driving force of applied electrical potential. After electrolysis was finished, the anode solution was filtered to remove excess silica. The remaining tungstate ions and Si^{4+} ions yield a pure polycrystal of TAS. The filtered solution was then evaporated in a steam bath, above 50–60°C, until a few crystals began to form.

2.2. *Composition Analysis of TSA*

The sodium content, the iron content, and the atomic ratio Si:W of the TSAs were measured by flame spectrophotometry, spectrographic analysis, and the air–hydrogen chloride method, respectively. The concentration of the tungstosilicate ion $[Si(W_3O_{10})_4]^{4-}$ in the anode solution was determined by UV spectrophotometry.

2.3. *Properties and Structure of TSA*

The instruments employed included a Type 401 thermobalance, a Perkin–Elmer Type 577 IR spectrophotometer, a Type 240 UV–visible recording spectrophotometer, and a Rigaku-D/MAX-rA powder diffractometer. Anhydrous TSA powders were pressed into disks of 13× (35–48 mm); their conductivities were measured with an ac bridge method after their faces had been coated with gold under vacuum.

3. Results

3.1. *The Effect of Anode Solution pH on the Concentration of Tungstosilicate Ions* $[Si(W_3O_{10})_4]^{4-}$

As shown in Fig. 2, the $[Si(W_3O_{10})4]^{4-}$ ion begins to form at pH ~5.5, and its maximum concentration appears at about pH ~4.0. This is in accord with Ref. (*7*). In the pH range 4.0–0.4, the Na^+ ion can be removed further from the anode solution, even though the polyanion concentration drops slowly.

3.2. *Analysis and Detection of Fluorescently Pure TSA*

The following data were revealed by the above analytic and detecting methods: Na, $(3 \pm 2) \times 10^{-4}$; Fe, $(5 \pm 3) \times 10^{-7}$; and Si:

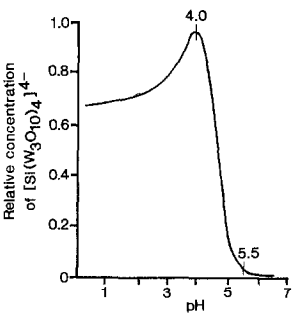

FIG. 2. Effect of pH on $[Si(W_3O_{10})_4]^{4-}$ concentration.

W = 1.00:11.98. The last value can be compared with the Si:W ratio of 1.00:12.00 for the theoretical value of the TSA $H_4[Si(W_3O_{10})_4]$, and the second value can be contrasted with the value $\leq 10^{-6}$ required by a luminescent host for trace impurity Fe. It can be reasoned that the TSA is a 12-tungstoheteropoly acid. This is in accord with the IR, UV, and X-ray diffraction data given below. The luminescent intensity of $Na_{5-x}Eu_{1-x}Si_x(WO_4)_4$ made up of this TSA, H_2WO_4(G.R.), Na_2CO_3(G.R.), Eu_2O_3 (99.95%). This luminescent material $Na_{5-x}Eu_{1-x}Si_x(WO_4)_4$ has not been reported before; we will discuss it in another paper. The purity of this TSA meets the specifications for fluorescent purity.

3.3. Certain Solid State Characteristics of TSA

3.3.1. Thermogravimetric (TG) analysis and thermodifferential analysis (DTA). It is seen from Fig. 3 that anhydrous TSA begins to decompose at 435°C; it decomposes completely at 525°C.

3.3.2. IR spectra and UV spectra. Except for the characteristic absorption peaks of the O–Si–O bond and the O–P–O bond, the solid state IR spectra (Fig. 4) and the solution UV spectra (Fig. 5) of TSA and tungstophosphoric acid are very similar.

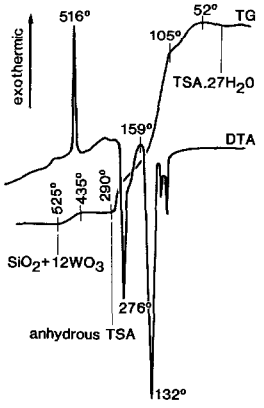

FIG. 3. TG and DTA curves of TSA.

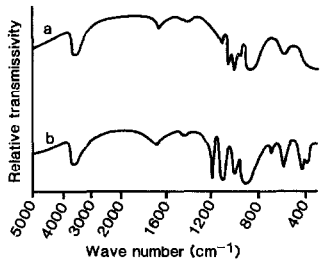

FIG. 4. IR spectra of TSA (a) and tungstophosphoric acid (b).

The absorption bands or peaks at 1700–1400, 1060–980, 570–420, and 1020 cm^{-1} in Fig. 4 belong to crystalline water, WO_3, the O–W–O bond, and the O–Si–O band, respectively. There are no absorption peaks characteristic of the solutions of the starting materials, Na_2WO_4 and Na_2SiO_3, but a peak characteristic of TSA in solution appears at 236.9 nm (Fig. 5). This shows that a heteropoly acid TSA has been formed. The relation of Na_2WO_4, $(NH_4)_2HPO_4$, and tungstophosphoric acid accords with that of Na_2WO_4, Na_2SiO_3, and TSA.

3.3.3. Corrosion and conductivity of the

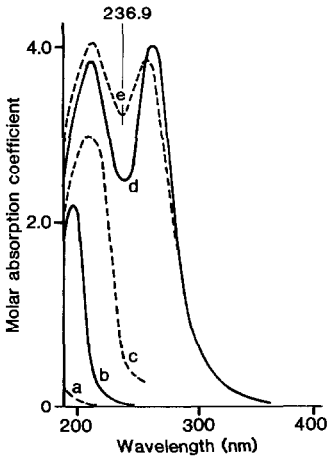

FIG. 5. UV spectra of 0.01 *M* Na_2WO_4 (a), 0.01 *M* $(NH_4)_2HPO_4$ (b), 0.01 *M* Na_2SiO_3 (c), 1×10^{-4} *M* $H_3[P(W_3O_{10})_4]$ (d), and 2×10^{-5} *M* TSA $(H_4[Si(W_3O_{10})_4])$ (e).

protons in solid state TSA. It was observed that a stainless-steel knife is corroded by solid state TSA, and a tungsten blue appeared on the knife when the knife was in contact with the TSA. This indicates that the protons in solid state anhydrous TSA have strong mobility and that solid TSA is a strong acid. At 25°C, its conductivity is $(3 \pm 1) \times 10^{-3}$ ohm^{-1} cm^{-1}, which shows that the corrosion has its own basis.

4. Discussion

4.1. Improvement on C.D. Vanderpool's Method by This Technique

4.1.1. By-product NaOH separated from the reactive system. During the electrolysis, the by-product NaOH solution flows continuously out of the negative side of the cell; with Vanderpool's method, NaOH is replaced by water only twice in each electrolytic synthesis.

4.1.2. Electrolytic solution kept at the same level. If deionized water is added to the electrolyzer continuously, the solution can be kept at the same level between the anode solution and the cation solution. With Vanderpool's method, however, the electrolytic solution cannot be kept so, since the anode solution volume decreases somewhat while the cathode solution volume apparently increases. The latter method has no means to keep the solution at the same level.

With these two improvements, the electrolytic reactions of the improved CEMEM was better controlled than with Vanderpool's CEMEM, so purer TSA is prepared.

4.2. High Thermal Stability and Solid Ionic Conductivity of TSA

Since the concentrations of trace poisonous impurities, such as Cl^-, Fe^{3+}, Sn^{2+}, Na^+, and K^+ in the TSA prepared with our technique are fairly low, its thermal stability is higher than that of other TSAs. For instance, both the initiation and complete decomposition temperatures are about 30°C higher than those of the TSA made by West and Audrieth (*8*).

Only one exothermic peak (516°C) appears in the temperature range 435 to 525°C on the DTA curve of the TSA. It may be reasoned that the endothermic effect of slowly decomposing anhydrous TSA is not seen; furthermore, crystallization of amorphous WO_3 and the decomposition of anhydrous TSA occur at almost the same temperature; thus, the exothermic effect of WO_3 crystallization is enhanced. The endothermic effect is mainly compensated for by the exothermic effect, which reveals the interdependence of the different heat effects.

The conductivity of anhydrous TSA is somewhat smaller than that of a superionic conductor ($\sim 10^{-2}$ ohm^{-1} cm^{-1}). It is suggested that the higher hydrates of TSA have higher conductivities because the hydrogen-bond network as a path of proton conduction would not be so well established in the anhydrous or lower hydrates as in the higher hydrates (*9*).

References

1. D. L. KEPERT, *Prog. Inorg. Chem.* **4,** 200 (1962).
2. L. P. KAZANSKII, E. A. TERCHENKOVA, AND V. I. SPITSYN, *Advanced Chem. (USSR)* **18,** 1139 (1974).
3. S. V. BALTIUKOVA, T. V. KRAVCHELKO, AND L. I. KONONENKO, *Dokl. Akad. Nauk. USSR* **242**(6), 1340 (1978).
4. J. C. CHERMAN, C. JASMIN, M. GEORGES, AND R. MARCEL, *Ger. Offen.* 2,064,296, July 15, 1971.
5. C. D. VANDERPOOL, J. C. PATTON, JR., TAI K. KLM, AND M. B. MACINNIS, U.S. Patent 3,947,332, March 30, 1976.
6. V. CHLOLA AND C. D. VANDERPOOL, U.S. Patent 3,361,518, Jan. 2, 1968.
7. J. C. BAILER, JR., *et al.* (Eds.) *in* "Comprehensive Inorganic Chemistry," Vol. 4, p. 649 Pergamon, Elmsford, NY (1973).
8. S. F. WEST AND L. F. AUDRIETH, *J. Phys. Chem.* **59,** 1069 (1955).
9. O. NAKAMURA AND I. OGINA, *Mater. Res. Bull.* **17,** 231 (1982).